



OPEN Generation of arbitrarily patterned polarizers using 2-photon polymerization

Byron Ganazhapa^{1,2✉}, Javier Pereiro-García¹, Xabier Quintana Arregui¹, Morten Andreas Geday¹, Gonzalo Guadaño² & Manuel Caño-García^{1,3}

Patterned polarizers are prepared using liquid crystals (LC) doped with a black dichroic dye and in combination with a linear polarizer. The pattern is achieved with a nanostructured LC alignment surface, that is generated using a two-photon polymerization direct laser write (2PP-DLW). This technique creates a pattern of high-resolution grooves in the photoresist at any arbitrary angle. The angle governs the LC orientation at any substrate surface point, determining the transmitted light linear polarization angle. This paper presents the first use of a 2PP-DLW cured positive tone photoresist for dichroic dye-doped LC alignment. Two complementary photoresists have been employed: conventional negative tone SU-8 photoresist and, in this context novel, positive tone S1805 photoresist. The alignment quality of the polarizers has been assessed by analyzing the transmission using an additional polarizer. For SU-8, the resulting grayscale pattern and a contrast ratio (CR) of 14 has measured. The uniformity of the alignment has been measured to be 65% using normalized Shannon entropy (H). For S1805, a CR of 37 was measured, and a uniformity of 63% was obtained. 2PP-DLW allows for shaping complex patterns in submicron dimensions and for the fabrication of arbitrarily patterned polarizers and other LC devices.

Liquid crystals (LC) surface alignment is commonly employed to control the LC molecular orientation^{1,2}. Photo-alignment techniques may be used to generate customized patterns in the aligning surfaces^{3–7}. The resulting LC or polymerized reactive mesogens films may serve in various applications, such as spatial geometric phase modulators or polarization holograms⁸, since the alignment layer provides precise control of 2D and 3D molecular orientation in LC cells⁹. Adding dichroic dyes or fluorescent dyes to the LC broadens the application range^{4,10–13}.

The direct laser writing (DLW) technique may be employed for curing of photosensitive materials, creating micrometric structures that may align LC molecules^{14–16}. Two-photon polymerization DLW (2PP-DLW) enhances the dimensional characteristics of 2D and 3D microstructures with nanometric resolution^{17–20}.

Several 2PP studies have focused on studying the behavior and quality of LC alignment surfaces^{21,22}, aiming to enhance the optical properties of cholesteric LCs (CLC)²³ and explore innovative techniques for alignment in 3D structures in LC cells^{15,24}. Pavlov et al.²⁵ demonstrated surface alignment on titanium (Ti) layers composed of periodic grooves of 920 nm through 2PP-DLW, using a powerful laser to generate alignment surfaces for nematic LCs, with strong anchoring. Jagodič et al.²¹ showed good LC alignment in complex patterns on thin layers of commercial negative tone photoresists. Additionally, Ji et al.²⁶ developed a compartmentalized alignment method of polymeric ribbons in LC to produce relief gratings on surfaces, creating arbitrary configurations of curved shapes and checkerboard-type patterns in microstructures.

2PP-DLW was used to modify the morphological geometry of LC structures²⁷. Notably, Lee et al.²⁸ designed and surface-aligned multi-layered LC cells (2–3 layers) to create 3D spatial light modulators, resulting in significantly improved response times when compared to conventional single-layer counterparts. Sandford et al.²² developed a compact and transmissive multi-layer polymer-based LC device with 3D switching, generating holograms by voltage-induced modulation. Configurable patterns for image encryption and encoding through 2PP-DLW in LCs have been used in authentication and security applications. For instance, Tartan et al.²⁹ employed a rewriting technique with ultrashort pulsed lasers and voltage applied to encode the features of a fully assembled polymerizable LC. Meanwhile, Van Winkle et al.³⁰ proposed a pattern reconfiguration technique for

¹CEMDATIC, ETSI Telecomunicación, Universidad Politécnica de Madrid, Av. Complutense 30, Madrid 28040, Spain.

²LASING S.A, c/Julián Camarillo, 26, Madrid 28037, Spain. ³Department of Electronics and Computer Technology, Research Centre for Information and Communication Technologies (CITIC-UGR), University of Granada, Granada, Spain. ✉email: b.ganazhapa@upm.es

intrinsic non-binary information encoding using polarizers. This method modulated light intensity in doped regions of LCs with donors/acceptors written at polarization angles on their surfaces and erased through heating.

Studies combining photo-alignment and 2PP-DLW to align LC surfaces have been undertaken. Shi et al.¹⁴ used a uniform UV exposure to orient a liquid crystalline conjugated polymer, and 2PP-DLW employed to write patterns in a dye, successfully transferring patterns to the film through thermotropic reorientation and solidification at room temperature. These advancements underscore the versatility and potential of 2PP in the realm of surface alignment and LC-based device manufacturing.

In applications involving complex alignments in LC, particularly in the context of the geometric phase known as the Pancharatnam-Berry (PB) phase, several studies have centered on planar optics devices. e.g. compact see-through near-eye displays³¹, augmented reality (AR) near-eye displays based on PB phase lenses³², holographic CLC reflective lenses with high efficiency and polarization selectivity³³, coexisting superstructures with opposite chirality for PB phase inversion in CLCs (generating reflective optical vortices)³⁴, and 2D geometric-phase liquid crystal diffraction gratings (generating arrays of equi-energetic optical vortices)³⁵. These devices, many of which are already employed in the industry and are costly to manufacture using conventional techniques³⁶, can be produced with 2PP-DLW technique at a lower cost, with increased reliability in complex alignment³⁷.

In this work, arbitrary surface alignment was introduced using both negative and positive tone photo resist to create polarizer patterns using 2PP-DLW. The assembled cells are based on nematic LCs, with black dichroic dyes. The contrast ratio (CR) and entropy (H) for alignment quality have been assessed employing additional standard polarizers.

Experimental

Methods and materials

Commercial 0.7 mm-thick glass ITO coated slides are used as substrates. The indium-tin oxide (ITO) layer is nominally 130 nm-thick and provides good and uniform adherence of the photosensitive material. Additionally, the high refractive index contrast with the prepolymer ($n \approx 1.6$) and the ITO ($n \approx 1.8$) covered glass substrate facilitates the focusing of the laser for selective curing, although in this work since the complete layer of prepolymer is five times less than the voxel depth, the focusing may be done on the air-prepolymer interface using a 50 \times microscope objective lens with numerical aperture of 0.80, as shown in Fig. 1 and Figure S1. Negative-tone and positive-tone photoresists can selectively be polymerized or decomposed using two-photon absorption (2PA). An explanation of 2PA mechanism is described in the Supplementary Information. The patterned alignment surface for the LC is fabricated using a custom-built equipment described in Figure S2 and Table S1 of the provided Supplementary Information. The 2-photon polymerization (2PP) setup description is provided by Lasing S.A.³⁸.

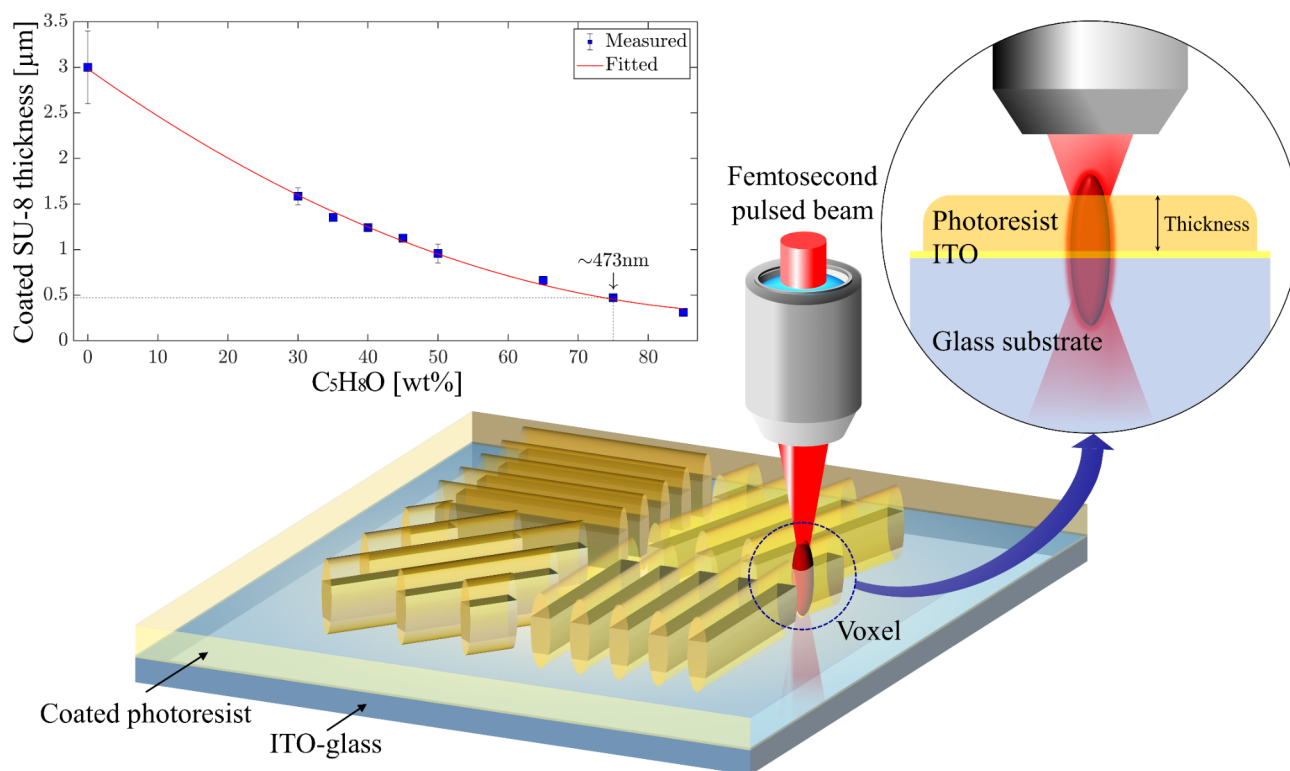


Fig. 1. Schematic illustration of photoresist orientation using the two-photon polymerization direct laser writing (2PP-DLW). The inset shows the thickness of SU-8 photoresist spin-coated onto an ITO-glass substrate.

Prior to 2PP-DLW meticulous cleaning process is carried out. First, the substrate is cleaned with lint-free cloths and immersed in 2-propanol/acetone for 1 min. Subsequently, ultrasonic cleaning is performed for 30 min in deionized water. Afterwards, the substrate is thoroughly rinsed with deionized water and dried with nitrogen flow. Finally, high-temperature baking at 200 °C for 120 min eliminates any remaining adsorbed water. Before dispensing the photoresist onto the glass surface, the substrate is placed under deep ultraviolet light (UVO-Cleaner) for 10 min to eliminate any organic material. This step also makes the substrate surface more hydrophilic, improving the adhesion of the deposited photoresist.

Photoresist is drop-casted onto the ITO-glass substrate (1 ml of photoresist for each 25 × 25 mm² substrate) for spin-coating. Two different types of photoresists were used: SU-8 TF 6002 (SU-8) negative-tone photoresist (Kayaku Advanced Materials) and the S1805 G2 (S1805) positive-tone photoresist (Shipley), both obtained from Micro Resist Technology GmbH. SU-8 is mixed with cyclopentanone (C₅H₈O) solvent to reduce the viscosity of the photoresist. A mixture containing 75 wt% of C₅H₈O is used to achieve a thickness of ~0.5 μm, as shown in the inset of Fig. 1. To get to this thickness the solution is spin-coated at 3000 rpm for 30 s with acceleration ramps of 500 rpm/s.

S1805 is spin-coated as supplied at 3500 rpm for 30 s with acceleration ramps of 500 rpm/s to achieve 0.5 μm thickness. Finally, the photoresist is soft-baked at 115 °C for 1 min to get it ready for the 2PP-DLW. Spin-coating parameters of both photoresists are summarized in Table 1.

Alignment of LC by 2PP photoresist

As mentioned above SU-8 has previously been used for LC alignment^{26,27}. Upon polymerization, it generates a well-defined 3D nanostructure with high resolution and a high aspect-ratio once exposed to the laser beam^{39–41}. It exhibits high resistance to solvent, while the unexposed portion is highly soluble in developing solutions. S1805 is efficient in manufacturing hollow lines, requiring relatively small insolation energy and easy removal of the exposed part of the material when developed⁴².

The S1805 results in structures inverse to those generated with SU-8 when the same exposure pattern is used. Both may serve as direct aligning patterns or as master molds for creating, via nanoimprint, LC alignment surfaces in other materials^{17,19}. Both photoresists share the property of being practically transparent in the visible spectrum⁴³. Furthermore, SU-8, is thermally stable^{20,42}.

2PP-DLW is governed by applying an appropriate energy dose during the exposure. The laser exposure energy is optimized to the polymerization threshold levels and is achieved by adjusting the focal spot travel speed in the XY-plane and controlling the laser power. This process ensures the generation of truncated voxels (see Fig. 1). In our setup for a xy-voxel size of approximately 0.5 μm, the printing parameters for SU-8 were a scanning speed of 1 mm/s and 78 mW of average laser power (energy of 0.975 nJ/pulse). For S1805, a scanning speed of 6 mm/s at 42 mW (0.525 nJ/pulse) was optimal. These parameters ensure that the exposure energy applied is appropriate to polymerize the entire thickness of the photoresist.

To execute the polymerization process, the designed patterns are loaded and programmed on a customized software (Lasing Processing Software) provided by Lasing S.A.³⁸. The laser spot is focused onto the ITO-photoresist interface (XY focal plane of the objective lens, see Fig. 1). In the case of SU-8, the sample is post-baked at 115 °C for 4 min after the exposure in order to complete the cross-linking process. The S1805 does not need any postbake, although it can be used to harden unexposed photoresist before the developing process.

Finally, the substrates are developed by submerging them into photoresist developer (PGMEA developer for SU-8 and Metal Ion-Bearing developer for S1805) for 10 s and 30 s respectively, then cleaned for 30 s (2-propanol for SU-8 and deionized water for S1805), and dried using nitrogen flow.

The post-exposure processes used in this work are determined empirically and summarized in Table 1. The topology of alignment layer has been analyzed using a field emission scanning electron microscope SEM (EVO 10, ZEISS group). Prior to imaging, a 100 nm thick layer of gold was deposited on all polymerized photoresist, and an electron beam voltage of 8 kV was applied at a working distance of 7.661 mm (Fig. 2a), 6.05 mm (Fig. 2b), and 15.11–19.91 mm (Fig. 2c). The photoresist exhibited perfectly polymerized lines with a repetitive periodicity (~1 μm) in all directions, as depicted in Fig. 2a–b. In Fig. 2c, perfectly defined lines are observed in the printing directions of 0 and π/2 radians (90°) on both photoresists, while in the other directions, lines exhibit slightly less perfection. The presented results show patterns with grooves of 0.5 μm width and polymer lines with a depth of 0.5 μm, and a pitch of 1 μm. These structures enable the arbitrary surface alignment of patterned LC in this work.

LC patterning devices

Patterned polarizers have been prepared with the 2PP-DLW printing lines at different angles defining the molecular orientation (φ). Nematic LC (5CB, Merck) doped with 2.0 wt% of black dichroic dye (D8, Mitsui

Material	Spin-coating parameters				Baking parameters	
	steps	Speed (rpm)	Acceleration (rpm/s)	Time (s)	Soft-bake	Post-bake
SU-8 + C ₅ H ₈ O	1/2	500	100	5	1 min at 115 °C	4 min at 115 °C
	2/2	3000	500	30		
S1805	1/1	3500	500	30	1 min at 115 °C	4 min at 115 °C
PI2525	1/2	500	100	5	5 min at 80 °C	60 min at 250 °C
	2/2	2500	500	30		

Table 1. Spin-coating parameters of photoresists and polyimide deposition.

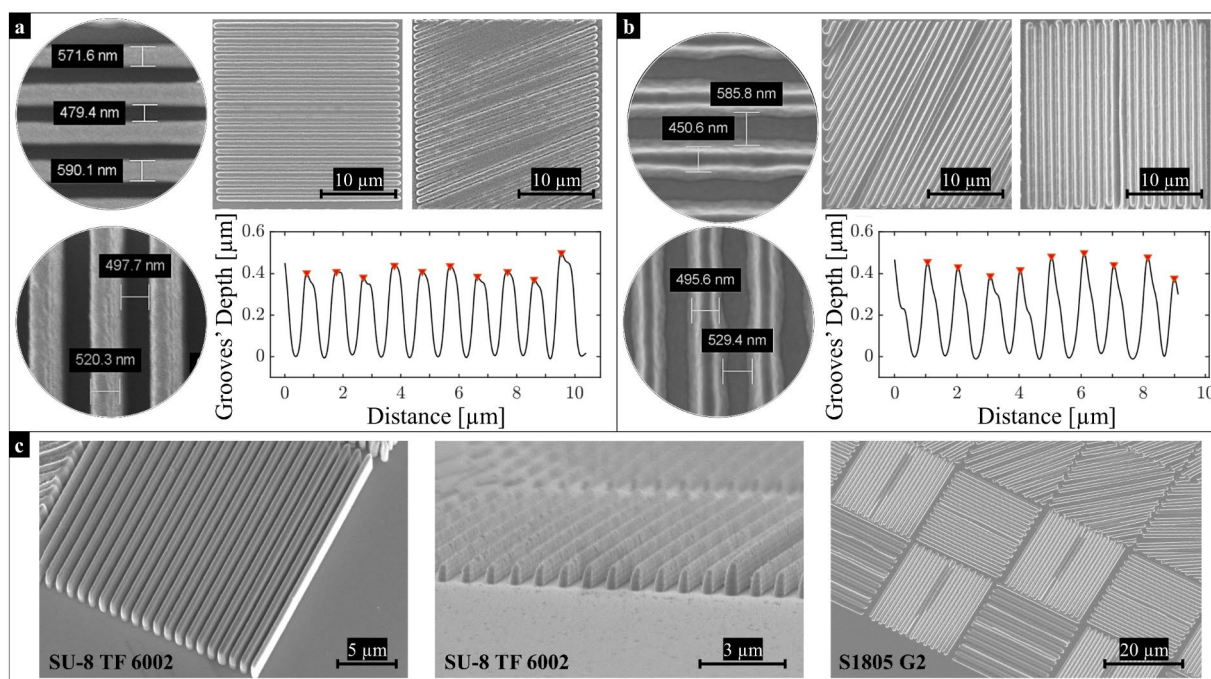


Fig. 2. SEM images of aligned surfaces of patterned lines at different angles of the 2PP-DLW printing direction. (a) Polymerized line patterns in directions of 0 and $\pi/9$ (20°) on SU-8 photoresist. (b) Polymerized line patterns in directions of $\pi/3$ (60°) and $\pi/2$ (90°) on S1805 photoresist. (c) 3D visualization of the printed patterns for both photoresists.

Chemical Inc.) was used. Cells were fabricated by assembling two ITO-glass substrates. One of the substrates is patterned using 2PP-DLW, while the other is coated unidirectionally rubbed polyimide (PI2525) to achieve a homogeneous planar orientation. The polyimide is spin-coated to obtain an average 200 nm uniform layer thickness, followed by soft-baking at 80 °C for 5 min, and cured by post-baking at 250 °C for 60 min. The spin coating conditions for all aligning surfaces are listed in Table 1.

A simple cell structure with an LC alignment pattern is shown in Fig. 3a, where 2PP-DLW printed line directions are shown on the lower substrate, while the polyimide rubbing direction is indicated on the top substrate. The 2PP-DLW aligned LC molecules, parallel to the grooves in the lower substrate, and the LC molecules aligned parallel to the rubbing direction on the top will generally cause twist orientations of the LC in different patterns of the cell. This configuration resembles to some extent a conventional twist-nematic cell⁴⁴, although the device is actually a guest-host system⁴⁵.

The cell gap was determined by silica beads spacers of 14 μm. The cells were filled with the LC and sealed and examined under a polarized microscope (MDi8, Leica) equipped with a calibrated digital camera (D3400, Nikon) and standard linear polarizers.

The contrast ratio (CR), and entropy (H) of grayscale levels for each LC cells have been determined by analyzing the images captured by the camera. To assess the alignment quality and maximum CR, independently of the dichroic dye, the cells are also examined between two standard polarizers.

Results and discussions

Alignment patterns with a pitch (Pt) of 1 μm and a linewidth (A) of ~ 0.5 μm in 25×25 μm² area per pattern as shown in Fig. 3a were employed. The chosen line aspect ratio, width and pitch has previously been employed in the group for nano-imprint alignment of LC. The lines of a printed pattern were generated using vectorial plotting at any given alignment angles (φ) resulting in nicely defined structures as seen in Fig. 2.

Cells with dichroic dye-doped LC, mounted as sketched in Fig. 3a, scale transmission images when linearly polarized light is incident on the 2PP-patterned surface. The uniformly rubbed surface, with known LC alignment direction, permitted the confirmation that absorbing polarization and the LC director coincided. When then alignment angle of the LC (φ), and thus the guest dichroic dye, coincides with that of incident light polarization, minimum light will be transmitted⁴⁵, while if the incident polarization is perpendicular to the alignment angle a maximum of light will be transmitted. For any other φ an intermediate fraction of the light will be transmitted. This observation also allowed for an absolute alignment direction assignment of the LC molecules on the nanostructures.

In all the below figures, LC alignment angle (φ) is indicated, not the light transmitted by the LC.

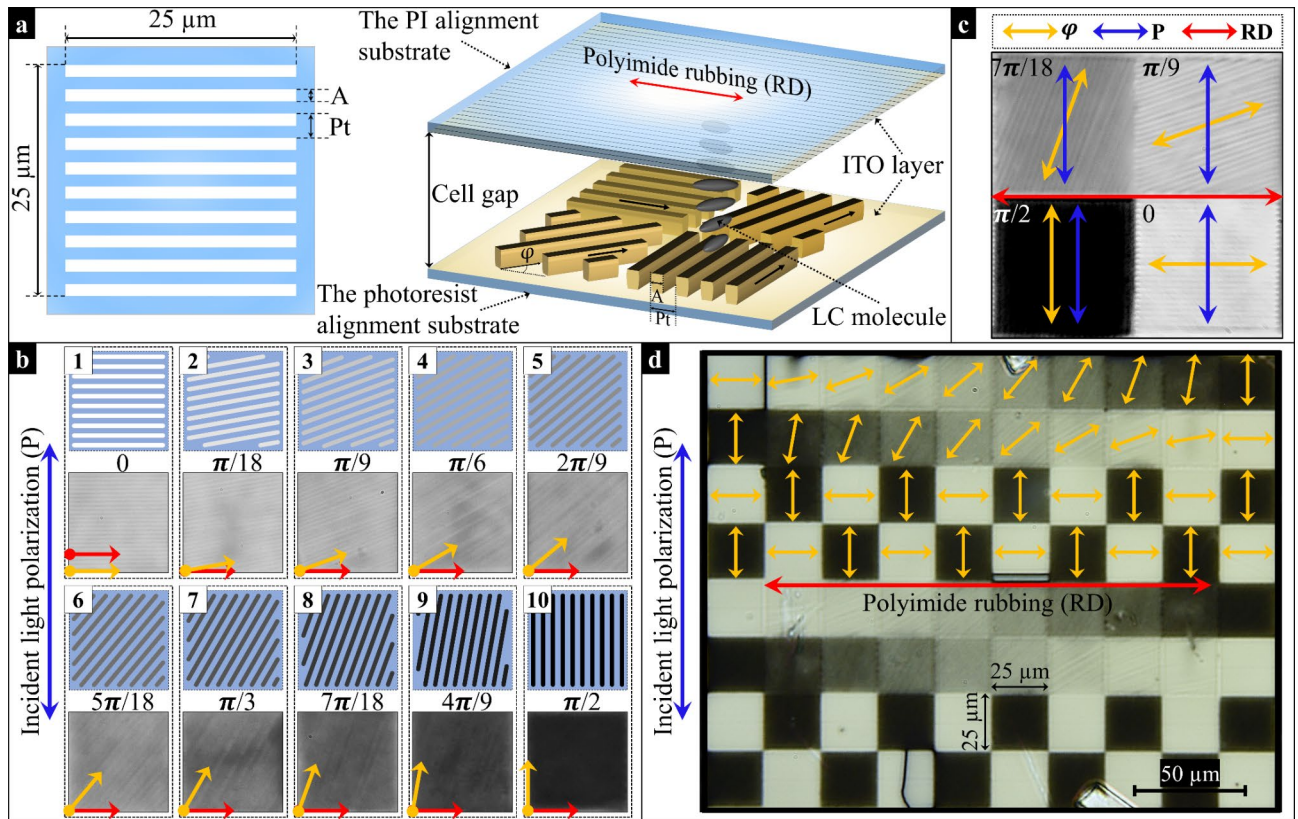


Fig. 3. Dichroic LC patterned polarizer. **(a)** Definition of pitch Pt and linewidth A and representation of an assembled LC cell. **(b)** Comparison of a set of the 10 patterns of a SU-8 aligned patterned polarizer that defines 10 grayscale levels in LC cells as a function of the alignment angles (φ) with incoming vertical polarization for all patterns. **(c)** Micrographs of a SU-8 aligned patterned polarizer with the polarization axis of an incident light (P) to the 2PP structures of four patterns with different angles φ . The polyimide rubbing direction of the other substrate (RD) does not affect the transmission of the light with incoming vertical light polarization. **(d)** Micrograph of the entire pattern employed in the dichroic dye-doped LC cell with chessboard pattern and the 10-step grayscale repeated twice. All micrographs were taken with the patterned polarized backlight with vertically polarized light.

SU-8 photoresist

In this study, 10 distinct patterns of parallel lines have been defined and printed under identical conditions. Each pattern, n , is characterized by an alignment angle $\varphi_n = \left(\frac{\pi}{18}\right) \times \{(n-1) | 1 \leq n \leq 10\}$, as shown in Fig. 3b. The 10 different φ_n values result in varying light transmission of the assembled cell when illuminated by linearly polarized white light from the patterned side. The nanostructured texture is reflected in visible variations in the light transmission, confirming that the dye and LC are aligning parallel to the engraved lines, as seen in previous studies^{26,27}.

The 2PP structure in SU-8 exhibits good alignment of the LC with a high repeatability in all directions uniformly across the individual alignment patterns (Fig. 3b-c). The grayscale transmission obeys Malu's law, as shown in the supplementary information. In Fig. 3d, a patterned polarizer with patterns arranged in a chessboard-like configuration is shown, together with ascending/descending grayscales. A visible edge between adjacent patterns can be appreciated, corresponding to the inter pattern space in the design as seen in Fig. 3a.

The quality of the patterned polarizers in the LC cells has been quantified by the contrast ratio (CR)²¹. The transmitted light intensities were quantified using a NIKON D3400 camera configured with sensibility ISO-400, with exposure time of 1/125 s and 1/30 s. Subtracting the average minimum intensity transmitted by the standard crossed polarizers, denoted as (\bar{I}_{bkgr}), with the microscope precisely focused onto a glass surface, the following CR was calculated:

$$CR = \left(\bar{I}_{max,meas} - \bar{I}_{bkgr} \right) / \left(\bar{I}_{min,meas} - \bar{I}_{bkgr} \right) \quad (1)$$

where $\bar{I}_{max,meas}$ is the average transmitted light intensity by the brightest pattern, and $\bar{I}_{min,meas}$ is the minimum average transmitted light intensity by the darkest pattern. This resulted in a normalized CR of 14 for SU-8.

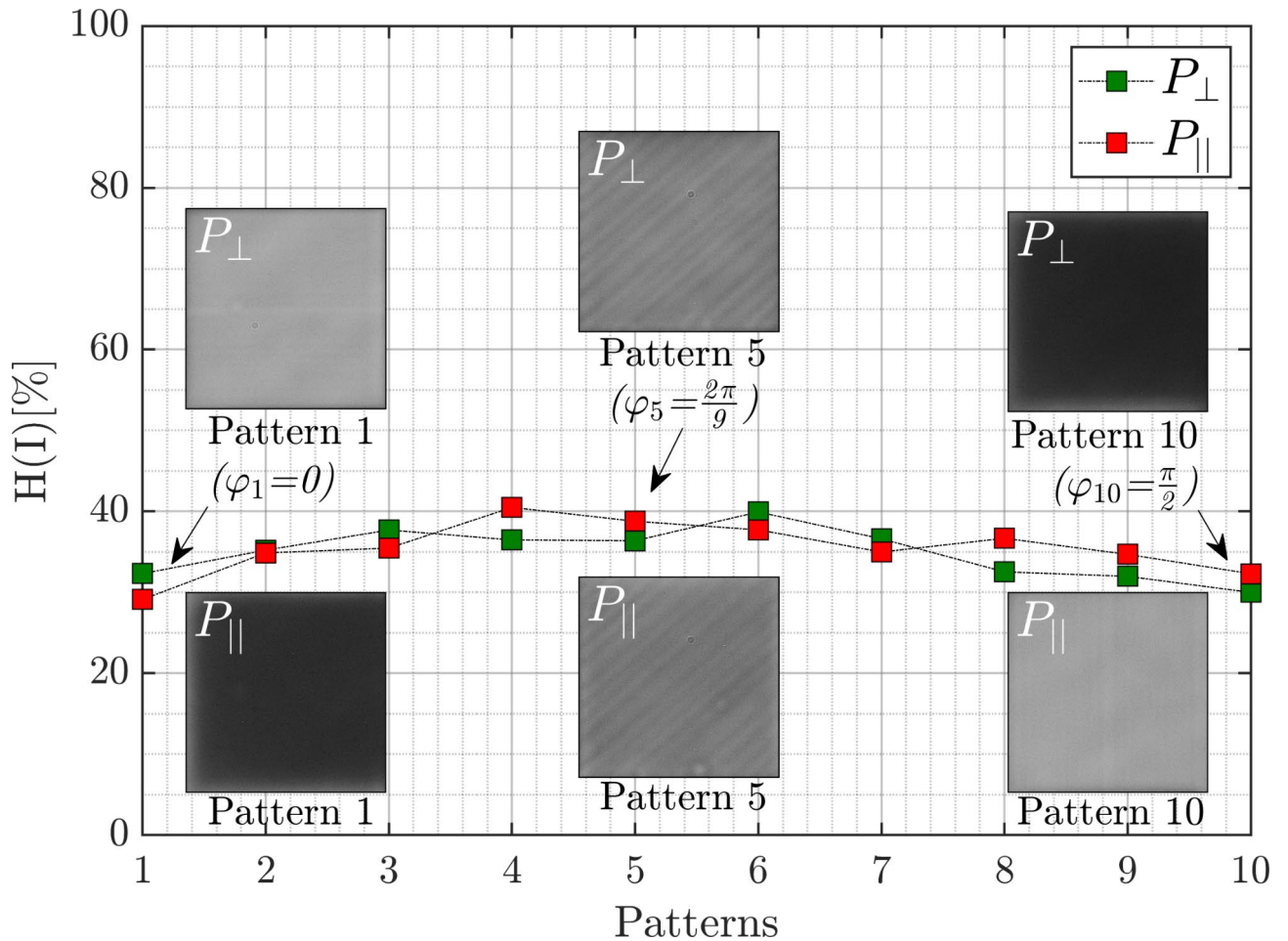


Fig. 4. Grayscale pattern entropy (H) of dichroic dye-doped LC cell in SU-8 aligned patterned polarizer. Parallel polarization (P_{\parallel}) and crossed (P_{\perp}) of the standard polarizer with respect to the rubbed substrate.

The uniformity of the pattern in the LC cells has been analyzed by employing image entropy (H)⁴⁶. This parameter measures the disorder in the intensity distribution and provides insights into uniformity of the molecular orientation within the grooves formed after 2PP-DLW. The disorder is calculated using the Shannon expression:

$$S(I) = \sum_{I=0}^N P(I) \times \log_2(P(I)) \tag{2}$$

where $P(I)$ is the probability of the occurrence of intensity I within the pixel pattern area and N is the number of intensities measured within the same pixel pattern area.

Where, the uniformity distribution is normalized, dividing the $S(I)$ computed as disorder measured by the maximum entropy of pixel pattern $max(S(I))$ when all intensities are equally likely to occur ($P(I) = 1/N$). Thus (2) becomes:

$$H(I) = -\frac{S(I)}{\log_2(N)} \times 100\% \tag{3}$$

Here, $H \approx 0\%$ denotes perfect uniformity, while $H \approx 100\%$ a random intensity variation of the pixels in the image. Figure 4 shows that the uniformity of each of the 10-pixel patterns. All the patterns show similar disorder under both parallel and crossed polarization, although each introduce a different twist in the LC cell, indicating a strong azimuthal anchoring.

H was calculated over an area of $25 \times 25 \mu\text{m}^2$ corresponding to 200×200 pixels² per pattern. The degree of disorder H is approximately 35%, representing around 65% of the uniformity. All measured patterns had a variability of approximately 8.8%, highlighting a low uniformity distribution with a standard deviation ($StDev$) of ± 3.1 .

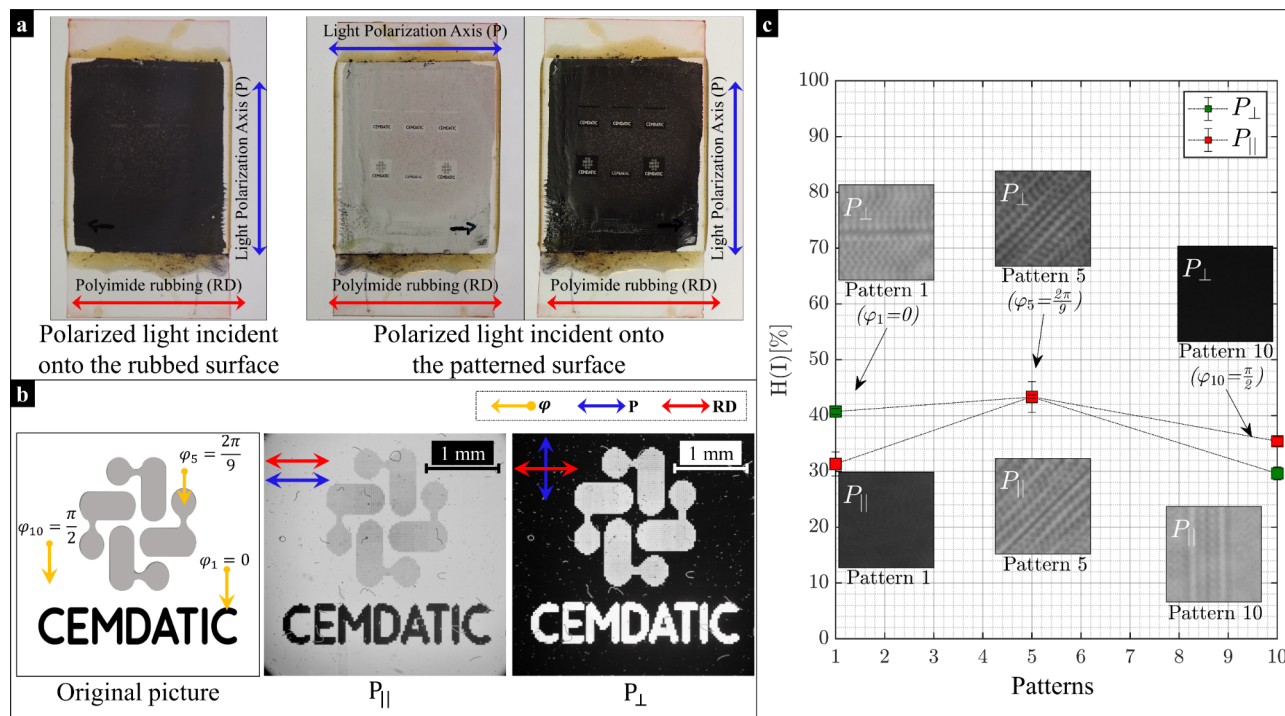


Fig. 5. Analysis of LC alignment fabricated in S1805. (a) Photos taken of the sample backlit with polarized light. Left: Light incident onto the uniformly rubbed surface. Middle and Right: Light incident onto the patterned surface, where recognizable features are clearly visible in separate aligned regions. (b) Original logotype used in the LC cell, and micrograph with a standard polarizer placed in parallel (P_{\parallel}) and crossed (P_{\perp}). The blue lines indicate standard polarizer (P) direction, red line indicate the polyimide rubbing direction (RD) of the polyimide and yellow lines indicate the alignment angle (φ) patterns. (c) Grayscale pattern entropy (H) of LC cell in S1805 aligned patterned polarizer.

Alignment Quality	SU-8 alignment	S1805 alignment
Normalized CR	14	37
Entropy (H)	$35 \pm 3.1\%$ 65% of uniformity	$37 \pm 5.3\%$ 63% of uniformity

Table 2. Alignment quality comparison (CR and H) for both SU-8 and S1805 alignment surface.

S1805 photoresist

The same cell structure and analysis have been performed on S1805. In Fig. 5, the LC alignment of a patterned polarizer with S1805 is shown. In this case a $3.2 \times 3.2 \text{ mm}^2$ logotype of CEMDATIC has been patterned instead of the checkerboard structure. The alignment of the LC molecules and dye is parallel to the orientation of the grooves cut in the S1805.

Figure 5a shows photos of the dichroic dye-doped LC cell backlit with polarized light incident onto the uniformly rubbed and patterned alignment surfaces respectively. The discrete 2PP aligned areas are clearly visible, with a visibly high contrast. In Fig. 5b, the original pixelated image and measurements of the transmitted light intensities in the doped cell are shown with the incident light polarization parallel to the alignment direction in the text (appearing dark text on bright background) or perpendicular hereto (appearing bright text on dark background). The normalized contrast ratio (CR) was of 37 for the measurements using (1).

As above the normalized Shannon entropy (H) of the intensity distribution of grayscale patterns, has been used to assess the alignment quality. In this case H was also calculated over an area of $25 \times 25 \mu\text{m}^2$ (200×200 pixels²/pattern).

Figure 5c shows the degree of disorder in the intensity distributions, approximately 37%, representing 63% of the uniformity in the doped LC. The measurements indicate a variability of approximately 14.2%, with a $StDev$ of ± 5.3 . The repetition rate of the laser pulses was too slow for the scanning rate, leading to imperfect alignment grooves. Even so the resulting structure aligned the LC. Table 2 presents a summary of the alignment quality for S1805 compared with its counterpart SU-8, both subjected to the same analysis conditions.

S1805 is an option for creating patterned polarizers in doped LCs. The patterning processes in large-sized LC cells is significantly faster in S1805 due to its high photo sensitivity (62 min of 2PP-DLW processing at a scanning speed of 6 mm/s) compared to SU-8 for the same CEMDATIC logotype (205 min at 1 mm/s).

Conclusions

The feasibility of achieving well-defined arbitrary alignment pattern has been confirmed through the creation of patterns of lines and grooves with a period of 1 μm and a height of 0.5 μm at different azimuthal printing angles (φ). This was accomplished using two complementary commercial photoresists, one, conventional SU-8, negative tone and one (S1805) positive tone. The high-resolution patterns were generated using Two-Photon Polymerization - Direct Laser Writing.

It is surprising that contrast ratio (CR) in the S1805 samples, is higher than that of the SU-8 aligned samples, especially when examining the inferior quality of the grooves made in S1805 (Fig. 5c). The interpretation of this result is that the interaction between the S1805 (a mixed cresol novolak-based resin), and LC molecules are much stronger than the interaction between SU-8 (an epoxy-based resin) and the LC.

Normalized Shannon entropy analysis was performed on the resulting pixels of patterns obtained from image processing. This measure depends directly on the uniformity, unlike the contrast ratio, that depends on the cell thickness, bulk order, and dye content.

SU-8 and S1805 are similar in both appearance and uniformity of the individual patterns (65% and 63% respectively), although the S1805 exhibited a slightly better contrast than SU-8. Thus, it is clear that the Shannon entropy cannot be employed as alignment quality measure on its own.

A novel way of assessing alignment quality has been presented. Furthermore, positive tone photoresist liquid crystal alignment has been demonstrated for the first time.

Data availability

Supplementary Information file is included in this article. Other data underlying the results presented in this paper may be obtained from the corresponding author (B.G.) upon reasonable request.

Received: 1 April 2024; Accepted: 23 September 2024

Published online: 29 September 2024

References

- Ishihara, S. & Mizusaki, M. Alignment control technology of liquid crystal molecules. *J. Soc. Inform. Display*. **28**, 44–74 (2020).
- Jones, L. P. Alignment properties of Liquid crystals. in *Handbook of Visual Display Technology* (eds Chen, J., Cranton, W. & Fihn, M.) 1387–1402 (Springer, Berlin, Heidelberg, https://doi.org/10.1007/978-3-540-79567-4_86. (2012).
- Yin, K., Xiong, J., He, Z. & Wu, S. T. Patterning liquid-crystal alignment for ultrathin flat Optics. *ACS Omega*. **5**, 31485–31489 (2020).
- Myhre, G. Patterned Liquid Crystal Polymer Retarders, Polarizers, and Sources. *Ph.D. Thesis*. The university of Arizona, (2012).
- Yan, Z. et al. Polarized optical properties in liquid crystals devices with photoaligned metal nanoparticle gratings. *Appl. Phys. A*. **127**, 82 (2021).
- Liu, D. & Broer, D. J. Liquid Crystal Polymer networks: Preparation, Properties, and applications of films with patterned Molecular Alignment. *Langmuir*. **30**, 13499–13509 (2014).
- Seki, T. New strategies and implications for the photoalignment of liquid crystalline polymers. *Polym. J.* **46**, 751–768 (2014).
- Kim, J. et al. Fabrication of ideal geometric-phase holograms with arbitrary wavefronts. *Optica OPTICA*. **2**, 958–964 (2015).
- Guo, Y. et al. High-resolution and high-throughput Plasmonic Photopatterning of Complex Molecular orientations in Liquid crystals. *Adv. Mater.* **28**, 2353–2358 (2016).
- Shen, W., Zhang, H., Miao, Z. & Ye, Z. Recent progress in functional dye-doped Liquid Crystal devices. *Adv. Funct. Mater.* **33**, 2210664 (2023).
- Fuh, A. Y. G., Chen, C. C., Liu, C. K. & Cheng, K. T. Polarizer-free, electrically switchable and optically rewritable displays based on dye-doped polymer-dispersed liquid crystals. *Opt. Express OE*. **17**, 7088–7094 (2009).
- Yu, B. H., Ji, S. M., Kim, J. H., Huh, J. W. & Yoon, T. H. Fabrication of a dye-doped liquid crystal light shutter by thermal curing of polymer. *Opt. Mater.* **69**, 164–168 (2017).
- Won, Y. et al. An electrically switchable dye-doped liquid crystal polarizer for organic light emitting-diode displays. *J. Mol. Liq.* **333**, 115922 (2021).
- Shi, Y. et al. Two-Photon Laser-Written Photoalignment Layers for Patterning Liquid Crystalline Conjugated Polymer Orientation. *Adv. Funct. Mater.* **31**, 2007493 (2021).
- Yang, Y., Wang, L., Yang, H. & Li, Q. 3D chiral Photonic nanostructures based on blue-phase liquid crystals. *Small Sci.* **1**, 2100007 (2021).
- Van Winkle, M., Scrymgeour, D. A., Kaehr, B. & Reczek, J. J. Laser rewritable dichroics through reconfigurable Organic charge-transfer liquid crystals. *Adv. Mater.* **30**, 1706787 (2018).
- Balena, A., Bianco, M., Pisanello, F. & De Vittorio, M. Recent advances on high-speed and holographic two-Photon Direct Laser writing. *Adv. Funct. Mater.* **33**, 2211773 (2023).
- Maruo, S., Nakamura, O. & Kawata, S. Three-dimensional microfabrication with two-photon-absorbed photopolymerization. *Opt. Lett. OL*. **22**, 132–134 (1997).
- Sun, H. B. & Kawata, S. Two-photon photopolymerization and 3D lithographic microfabrication. in *NMR • 3D Analysis • Photopolymerization* (eds Fatkullin, N. et al.) 169–273 (Springer, Berlin, Heidelberg, <https://doi.org/10.1007/b94405>. (2004).
- Harinarayana, V. & Shin, Y. C. Two-photon lithography for three-dimensional fabrication in micro/nanoscale regime: a comprehensive review. *Opt. Laser Technol.* **142**, 107180 (2021).
- Jagodič, U., Vellaichamy, M., Škarabot, M. & Mušević, I. Surface alignment of nematic liquid crystals by direct laser writing of photopolymer alignment layers. *Liq. Cryst.* **50**, 1999–2009 (2023).
- Sandford, O. et al. 3D switchable Diffractive Optical Elements fabricated with two-photon polymerization. *Adv. Opt. Mater.* **10**, 2102446 (2022).
- Yoshida, H. Functionalisation of cholesteric liquid crystals by direct laser writing. *Liquid Cryst. Today*. **21**, 3–19 (2012).
- del Pozo, M., Sol, J. A. H. P., Schenning, A. P. H. J. & Debije, M. G. 4D Printing of Liquid crystals: what's right for me? *Adv. Mater.* **34**, 2104390 (2022).
- Pavlov, I. A. et al. High-quality alignment of nematic liquid crystals using periodic nanostructures created by nonlinear laser lithography. *J. Mol. Liq.* **267**, 212–221 (2018).
- Ji, Z. et al. Compartmentalized liquid crystal alignment induced by sparse polymer ribbons with surface relief gratings. *Opt. Lett. OL*. **41**, 336–339 (2016).
- He, Z., Tan, G., Chanda, D. & Wu, S. T. Novel liquid crystal photonic devices enabled by two-photon polymerization [Invited]. *Opt. Express*. **27**, 11472 (2019).

28. Lee, Y. H. et al. Two-photon polymerization enabled multi-layer liquid crystal phase modulator. *Sci. Rep.* **7**, 16260 (2017).
29. Tartan, C. C. et al. Read on demand images in Laser-Written Polymerizable Liquid Crystal Devices. *Adv. Opt. Mater.* **6**, 1800515 (2018).
30. Van Winkle, M. et al. Direct-write orientation of charge-transfer liquid crystals enables polarization-based coding and encryption. *Sci. Rep.* **10**, 15352 (2020).
31. Lee, Y. H., Tan, G., Yin, K., Zhan, T. & Wu, S. T. Compact see-through near-eye display with depth adaption. *J. Soc. Inform. Display.* **26**, 64–70 (2018).
32. Moon, S. et al. Augmented reality near-eye display using pancharatnam-berry phase lenses. *Sci. Rep.* **9**, 6616 (2019).
33. Stebryte, M., Nys, I., Beeckman, J. & Neyts, K. Chiral liquid crystal based holographic reflective lens for spectral detection. *Opt. Express OE.* **30**, 42829–42839 (2022).
34. Zhu, L. et al. Pancharatnam–Berry phase reversal via opposite-chirality-coexisted superstructures. *Light Sci. Appl.* **11**, 135 (2022).
35. Marco, D., Sánchez-López, M. M., Cofré, A., Vargas, A. & Moreno, I. Geometric-phase grating as an optical vortex generator and detector. *Optical Sensing and Detection VI.* **11354**, 1135430 (2020).
36. BEAM Co. <https://www.beamco.com/>
37. Wang, Z., Wu, Y., Qi, D., Yu, W. & Zheng, H. Two-photon polymerization for fabrication of metalenses for diffraction-limited focusing and high-resolution imaging. *Opt. Laser Technol.* **169**, 110128 (2024).
38. Lasing, S. A. <https://www.lasing.com/>
39. Juodkazis, S., Mizeikis, V., Seet, K. K., Miwa, M. & Misawa, H. Two-photon lithography of nanorods in SU-8 photoresist. *Nanotechnology.* **16**, 846 (2005).
40. Qi, F., Li, Y., Tan, D., Yang, H. & Gong, Q. Polymerized nanotips via two-photon photopolymerization. *Opt. Express OE.* **15**, 971–976 (2007).
41. Teh, W. H., Dürig, U., Drechsler, U., Smith, C. G. & Güntherodt, H. J. Effect of low numerical-aperture femtosecond two-photon absorption on (SU-8) resist for ultrahigh-aspect-ratio microstereolithography. *J. Appl. Phys.* **97**, 054907 (2005).
42. Kayaku Advanced Materials, Inc. <https://kayakuam.com/>.
43. Biswas, S. Advanced processing of vertically aligned nanodevices. (2013).
44. Gooch, C. H. & Tarry, H. A. Optical characteristics of twisted nematic liquid-crystal films. *Electron. Lett.* **10**, 2–4 (1974).
45. Carrasco-Vela, C., Quintana, X., Otón, E., Geday, M. & Otón, J. Security devices based on liquid crystals doped with a colour dye. *Opto-Electron. Rev.* **19**, 496–500 (2011).
46. Sigaki, H. Y. D., de Souza, R. F., de Souza, R. T., Zola, R. S. & Ribeiro, H. V. Estimating physical properties from liquid crystal textures via machine learning and complexity-entropy methods. *Phys. Rev. E.* **99**, 013311 (2019).

Acknowledgements

This research was funded by the Comunidad de Madrid through the “PANTOMIME” (APOYO-JOVENES-21-9FOMOQ-22-0CNGFM), “DISEÑO Y FABRICACIÓN DE DISPOSITIVOS FOTÓNICOS” (BEAGALINDO-21-QU81R4-7-0QQBF3) and the “Ayudas para la realización de Doctorados Industriales de la Comunidad de Madrid” (IND2020/TIC-17424). The financial support to this study has also come from the Spanish Government, “ENHANCE-5G” (PID2020-114172RB-C22), “LC-LENS” (PDC2021-121370-C21), “DISRADIO” (TSI-063000-2021-83) and WOW-2D (PLEC2022-009381), as well as the Attract-IALL EU project G.A. 101004462 and “CONCEPT-2D” (G.A. 101062995), financed by the European Union. In addition, authors are grateful to the European Space Agency (ESA) for the financial support received with the “Smart Heaters” project (4000133048/20/NL/KML). M.C.G. is grateful to Spanish government grant (BG20/00136). The authors thank Prof. José Manuel Otón for his contribution in reviewing this article.

Author contributions

X.Q.A. and M.C.G. conceived the project and designed experiments. B.G. and X.Q.A. designed and manufactured the patterned polarizers. B.G. and J.P.G. carried out the measurements, data acquisition and analysis. B.G. and G.G. designed and built the custom 2PP system. B.G. wrote the manuscript and designed the figures and graphs. X.Q.A., M.C.G. and M.A.G. did the overall supervision. All authors reviewed the manuscript.

Declarations

Competing interests

The authors declare no competing interests.

Additional information

Supplementary Information The online version contains supplementary material available at <https://doi.org/10.1038/s41598-024-73946-z>.

Correspondence and requests for materials should be addressed to B.G.

Reprints and permissions information is available at www.nature.com/reprints.

Publisher’s note Springer Nature remains neutral with regard to jurisdictional claims in published maps and institutional affiliations.

Open Access This article is licensed under a Creative Commons Attribution-NonCommercial-NoDerivatives 4.0 International License, which permits any non-commercial use, sharing, distribution and reproduction in any medium or format, as long as you give appropriate credit to the original author(s) and the source, provide a link to the Creative Commons licence, and indicate if you modified the licensed material. You do not have permission under this licence to share adapted material derived from this article or parts of it. The images or other third party material in this article are included in the article's Creative Commons licence, unless indicated otherwise in a credit line to the material. If material is not included in the article's Creative Commons licence and your intended use is not permitted by statutory regulation or exceeds the permitted use, you will need to obtain permission directly from the copyright holder. To view a copy of this licence, visit <http://creativecommons.org/licenses/by-nc-nd/4.0/>.

© The Author(s) 2024